SMALL-ANGLE NEUTRON SCATTERING FROM
SDS MICELLES IN WATER

NIST – Center for Neutron Research
## NG3 Experiment - Summer School – June 2012

INTRODUCTION

Surfactants are amphiphilic molecules that form micelles in aqueous medium. The hydrophilic charged head groups associate with water while the hydrophobic tails aggregate inside the micelle core. Micelle structures have been well studied, using many characterization methods such as scattering, microscopy, and calorimetry.

Here, small-angle neutron scattering (SANS) is used to investigate the structure of SDS micelles in deuterated water and follow changes with SDS fraction and sample temperature; a range in SDS fractions and sample temperatures are discussed.

Sodium dodecyl sulfate (SDS) surfactant (99 % purity) was purchased from Sigma-Aldrich (St. Louis, USA) and D_2O (d-water) was purchased from Cambridge Isotope Labs (99.9 % purity). A series of SDS solutions were prepared for SANS measurements. Samples with the following SDS mass fractions were prepared: 0.1 %, 0.5 %, 1 %, 2 %, 5 %, 10 %, and 20 %. Three more samples were prepared where NaCl salt fraction was varied (0.1 mol/L, 0.2 mol/L and 0.5 mol/L) for the 1 % SDS/d-water sample. Samples were allowed to equilibrate overnight.

Preliminary SANS measurements were made using the NG3 30 m SANS instrument at the NIST Center for Neutron Research. Temperature was varied between 10 ^{o}C and 90 ^{o}C with 10 ^{o}C intervals. The actual sample temperature lagged behind the set sample block temperature. Standard overhead runs such as from the empty cell, the blocked beam as well as sample transmission and empty cell transmission runs were taken. SANS data were scaled to an absolute cross section using the empty beam transmission method. Standard data reduction method was used in order to obtain radially averaged intensity (units of cm^{-1}) as function of scattering variable Q (units of $Å^{-1}$). In this experiment, you will repeat this experimental procedure, analyze the data, and compare your results to these results and also to previously published results.
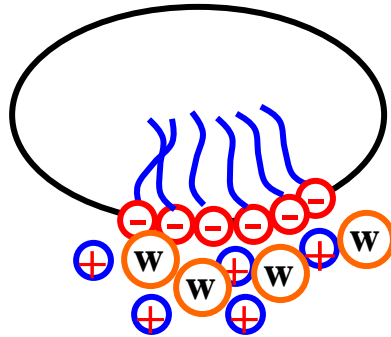
Figure 1: Schematic structure of an ionic micelle in water (w). The hydrated ionic head groups shield the hydrophobic tails of the surfactant from the water.

Table 1. Scattering length densities (SLD's) for SDS and water.

Material	Chemical Formula	Mass Density (g/ml)	SLD (Å^{-2})
SDS	$CH_3(CH_2)_{11}SO_4Na$	1.0	0.33×10^{-6}
Light water	H_2O	1.0	-0.56×10^{-6}
Heavy water	D_2O	1.105	6.36×10^{-6}

http://www.ncnr.nist.gov/resources/sldcalc.html

OBJECTIVES OF THE SANS EXPERIMENT

• Determine the shape and size of the surfactant micelles. How do the concentration and the temperature affect the aggregation?

• Determine the surface charge on the micelles. Again, how do the concentration and the temperature affect the charge distribution?

PREPARATION WORK BEFORE THE SUMMER SCHOOL

- Go over this handout carefully. Write down any questions you may have regarding the sample preparation, measurements to make, and the analysis of the resulting data.

- Read through or view the movies of the Fundamentals of SANS that are available at: http://www.ncnr.nist.gov/programs/sans/tutorials/index.html

- Understand the ellipsoid particle form factor and the MSA closure structure factor from the SANS Toolbox at: http://www.ncnr.nist.gov/staff/hammouda/the_SANS_toolbox.pdf

TRENDS OBSERVED IN SANS DATA

SANS data show a weak low-Q (long-range) feature and a dominant intermediate-Q (shorter-range) feature which is due to the micelle particles structure. The intermediate-Q peak and shoulder features observed in the SANS data are characteristic of anisotropic micelles such as ellipsoidal particles in agreement with previous results [Bergstrom-Pedersen, 1999]. These are seen to move to higher Q (Figure 2) upon heating implying that particles get smaller with increasing temperature. The low-Q feature (observed at low SDS fractions) is likely due to clustering and characterizes water-soluble (especially ionic) systems. At lower temperatures it may indicate the presence of hydrated SDS crystals. This low-Q feature has been discussed in the literature [Nieh et al, 2004; Hammouda, 2010]. It is characteristic of mass fractals (Porod exponents between 2 and 3).
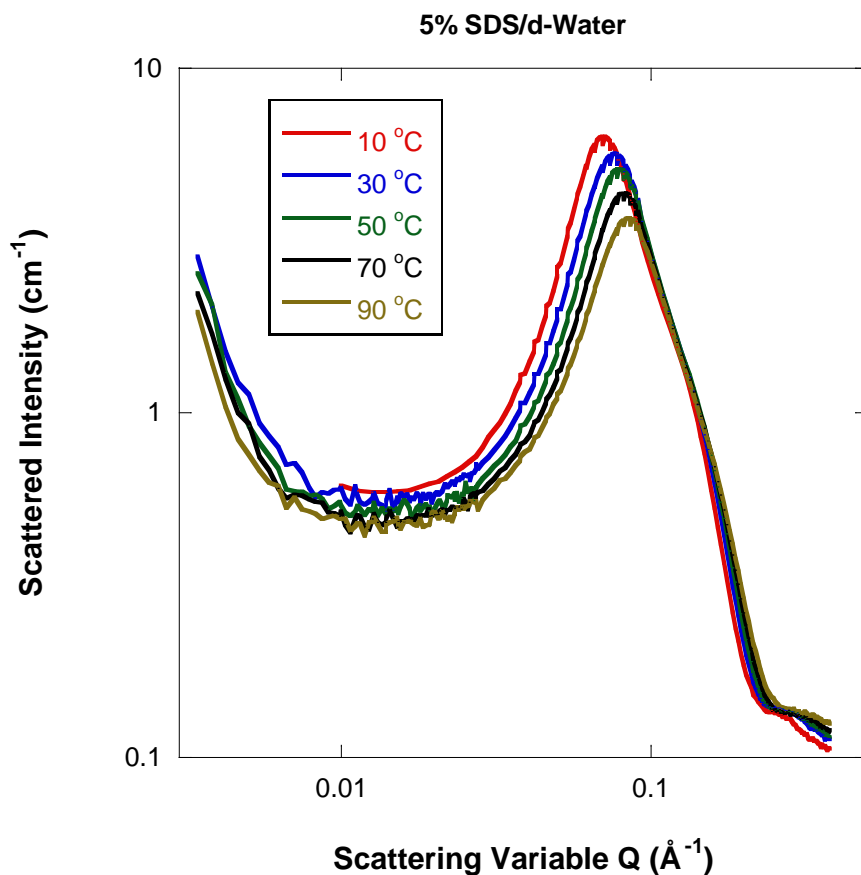
5% SDS/d-Water

Figure 2: SANS data for 5 % SDS mass fraction while varying temperature. The peak and shoulder features are characteristic of ellipsoidal micelles.

Increasing the SDS mass fraction for fixed high temperature (70 ^{o}C) shows smooth shape change for the ellipsoidal micelles. Only samples that are above the critical micelle formation concentration (i.e., at or above 0.5 %) are included in this trend. The peak and

shoulder features become more pronounced and move to higher Q (Figure 3), which means that the micelles become more ellipsoidal and their packing gets tighter.
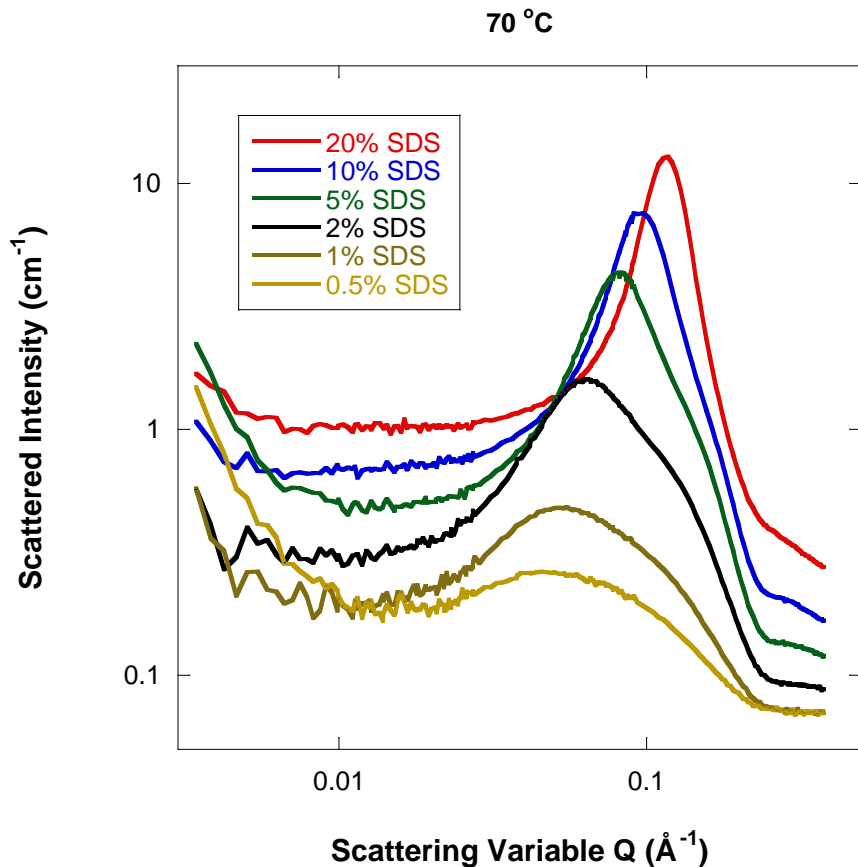
70 °C

Figure 3: SANS data for varying SDS mass fraction and a fixed temperature of 70 °C.

At the fixed low temperature of 20 °C, increasing the SDS mass fraction affects the SANS data more drastically. The low-Q feature is not pronounced till the SDS mass fraction becomes high enough (Figure 4). This feature characterizing long-range correlations between micelles becomes overwhelming for the 20 % SDS mass fraction sample. This 20 % SDS sample seems to contain another phase at 20 °C and below. The strong low-Q feature, smooth intermediate-Q peak variation and appearance of a high-Q shoulder are clues pointing to a two-phase system containing micelle particles as well as very large clusters. Visual inspection of this sample shows no macroscopic phase separation (no meniscus). Since no low-Q Guinier region was observed, the size of such clusters could not be estimated.
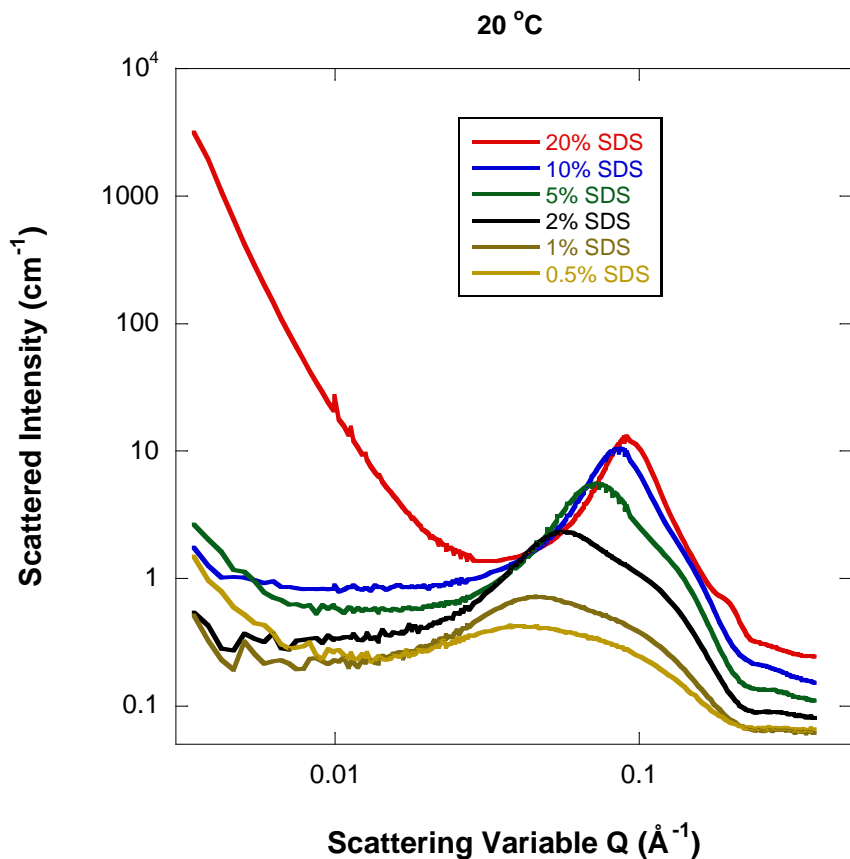
20 °C

Figure 4: SANS data for varying SDS mass fraction and a fixed temperature of 20 °C.

In order to investigate the low-Q feature further, SANS data for the 20 % SDS sample are plotted for the first three temperatures in Figure 5 (for 10 °C, 20 °C, and 30 °C). This feature is inexistent at 30 °C and is increasingly pronounced at lower temperatures. At 10 °C, a Bragg peak appears at high-Q. It is believed that at 10 °C, hydrated SDS crystals form in agreement with the previously reported phase diagram [Kekicheff et al, 1989] while at higher temperatures, ellipsoidal shape micelles dominate and SDS crystals have melted down. The Bragg peak defines the inter-lamellar d-spacing between the SDS-rich layers in the hydrated crystals separated by d-water layers.
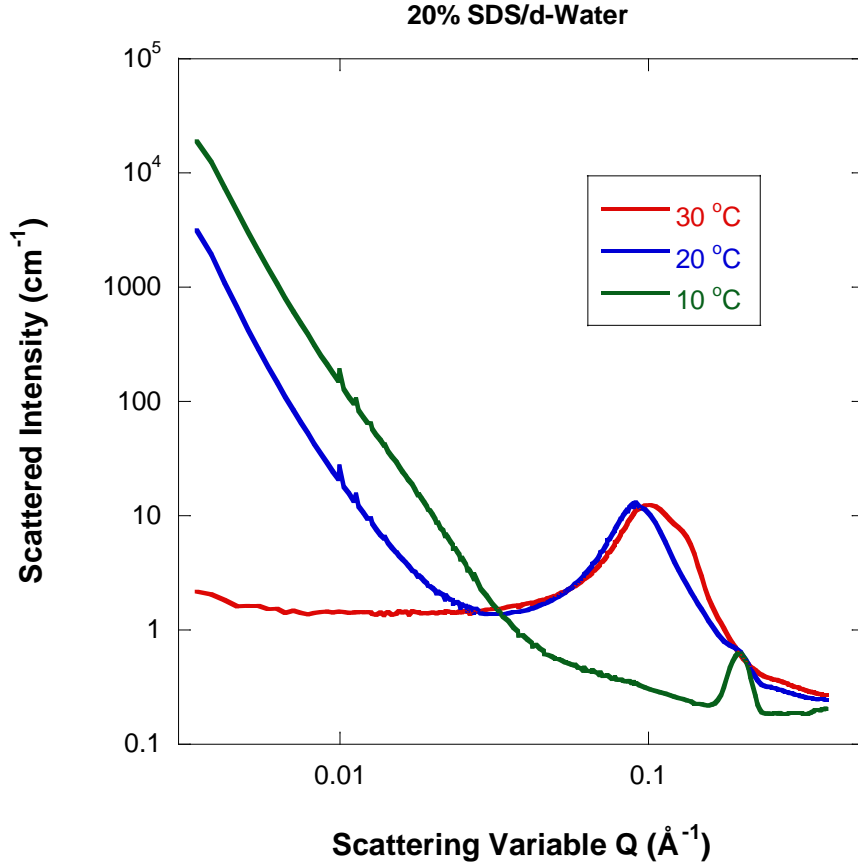
20% SDS/d-Water

Figure 5: SANS data for the three lowest temperatures for the 20 % SDS sample.

In order to obtain quantitative information, SANS data are fitted to a realistic scattering model described next.

SCATTERING MODEL

The recurring clues characterizing the SANS data consist of two size scales observed on the intermediate-Q peak. This points to ellipsoidal shape micelles as reported previously for similar systems [Borbely et al 1991; Prevost et al, 2009]. A scattering model consisting of a solution of interacting ellipsoidal particles is used to fit the SANS data. The scattering cross section is expressed as:

$$\left[\frac{d\Sigma(Q)}{d\Omega}\right]_{ellipsoids} = \Delta\rho^2\phi V_P P(Q)S_I(Q).\qquad(1)$$

Here $\Delta\rho^2$ is the contrast factor (see Table 1), ϕ is the particle volume fraction, V_P is the particle volume, $P(Q)$ is the single-particle form factor, and $S_I(Q)$ is the inter-particle structure factor. This model works best for spherical particles, and is used here for ellipsoidal particles that are not too distorted.

The form factor represents an average over orientations of the anisotropic particles. It involves the following integral:

$$P(Q) = \frac{1}{2} \int_{-1}^{+1} d\mu P(Q, \mu) .$$ (2)

Here $\mu = \cos(\theta)$ has been defined where θ is the angle between the main axis of the ellipsoid and the $\vec{Q}$ direction. Particles are assumed to be ellipsoidal with half axes R_a and R_b. For an oblate ellipsoid particle (with $R_b > R_a$), an effective radius R_e is defined as:

$$R_e^2 = R_b^2 + \mu^2 (R_a^2 - R_b^2) .$$ (3)

The form factor amplitude is the same as the one for a sphere of radius R_e:

$$P(Q, \mu) = \left[\frac{3 j_1 (QR_e)}{QR_e} \right]^2 .$$ (4)

Here $j_1 (QR_e)$ is the spherical Bessel function of order 1. Note that the orientations of single particles are assumed to be decoupled (valid for not too distorted particles and not too high particle fraction). With this caveat, the Mean Spherical Approximation (MSA) is used to model the structure factor $S_I(Q)$. This model is known to be reliable when screened Coulomb interactions are present (such as for ionic micelles), and relies on the MSA closure relation to solve the Ornstein-Zernike equation [Hayter-Penfold, 1981]. It should be mentioned that the approximate MSA model is often used since it relies on an analytical solution whereas other more elaborate (numerical) solutions are available. Fits to this model yield effective sizes.

The following model parameters are used: ε is the dielectric constant, D is the micelle (also called macroion) effective diameter, κ is the Debye-Huckel inverse screening length, and $z_m e$ is the electric charge on the micelle surface where e is the electron charge.

The Debye-Huckel screening parameter (inverse length) squared is expressed as follows:

$$\kappa^2 = \frac{e^2}{\varepsilon k_B T} \left(z_m \frac{\phi}{V_P} + \frac{\phi_{salt}}{V_{salt}} \right)$$ (5)

ϕ and ϕ_{salt} are the micelle particle and salt volume fractions, V_P and V_{salt} are the particle and salt molecule volumes, and $k_B T$ is the sample temperature in absolute units.

The micelle volume fraction ϕ is expressed in terms of the number density $\overline{N}$ and micelle volume $V_P = \pi D^3/6$ as $\phi = \overline{N}V_P$.

The MSA formalism used to derive the structure factor [Hayter-Penfold, 1981] is not reproduced here. This model is included in small-angle scattering data analysis software packages such as the IGOR-based package used at the NIST Center for Neutron Research. [Kline, 2006].

Note that the MSA model was originally introduced for spherical particles and is used here for ellipsoidal particles. This approximate approach should be reliable when the intermicelle distance is large compared to the micelle size.

In order to perform fits to the SANS data when sample temperature was varied, tabulated temperature dependence of the dielectric constant for d-water [Weast, 1984] is used (i.e., is fixed to help the fits). Table 2 reproduces such dielectric constants.

Table 2: Variation of the dielectric constant ε for deuterated water with temperature as tabulated [Weast, 1984].

Temperature (^{o}C)	10	20	30	40	50	60	70	80	90
Temperature (K)	283	293	303	313	323	333	343	353	363
Dielectric Constant	83.53	79.76	76.16	72.43	69.47	66.36	63.39	60.56	57.70

SANS DATA ANALYSIS

The model used to fit the SANS data consists of the sum of two functional forms: a low-Q power law function and the ellipsoidal micelle model:

$$I(Q) = \frac{A}{Q^n} + \left[\frac{d\Sigma(Q)}{d\Omega} \right]_{ellipsoids} + B . \qquad (6)$$

n is a low-Q Porod exponent, $\left[d\Sigma(Q)/d\Omega \right]_{ellipsoids}$ was discussed above and B is a constant representing the Q-independent background mostly due to incoherent scattering from hydrogen.

Smearing of the model was performed first using the SANS instrument resolution function. Then, nonlinear least-squares fits were performed on all SANS data sets. Fitting was reasonable in most cases despite the large number of fitting parameters. The resulting model parameters are: the low-Q scale factor A and Porod exponent n, the micelles volume fraction ϕ_{fit}, the ellipsoidal micelles half axes R_a and R_b, the scattering length

density inside the micelles ρ_m, the scattering length density for the solvent ρ_s, and the charge on the micelles. The sample temperature in absolute units was also fixed as well as the dielectric constant for d-water (Table 2). The contrast factor involves the difference $\Delta\rho^2 = (\rho_m - \rho_s)^2$ where ρ_m and ρ_s are the micelles and solvent scattering length densities respectively. Note that only this relative difference is relevant here.

A typical fit is shown in Figure 6 for the 5 % SDS mass fraction sample at 50 ^{o}C. The model used to fit reproduces the low-Q power law feature as well as hugs the intermediate-Q curve representing the oblate ellipsoidal micelles. The low-Q clustering feature is observed in most water-soluble systems.
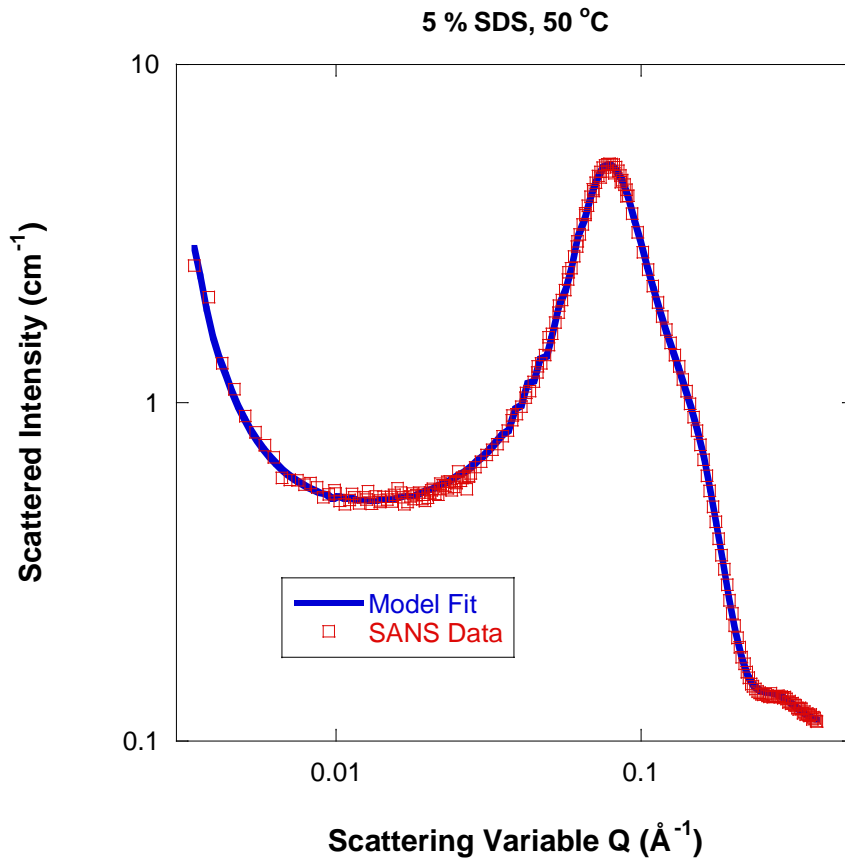
5 % SDS, 50 ^{o}C

Figure 6: Typical model fit and SANS data for the 5 % SDS/d-water sample at 50 ^{o}C.

Both ellipsoidal micelles half axes R_a and R_b decrease with increasing temperature as shown in Figure 7. The value of R_b was systematically larger than R_a pointing to oblate (i.e., compressed) ellipsoidal micelles as expected [Bergstrom-Pedersen, 1999;Yorelki et al, 2004]. Note that throughout this paper, error bars represent statistical precision and correspond to one standard deviation.
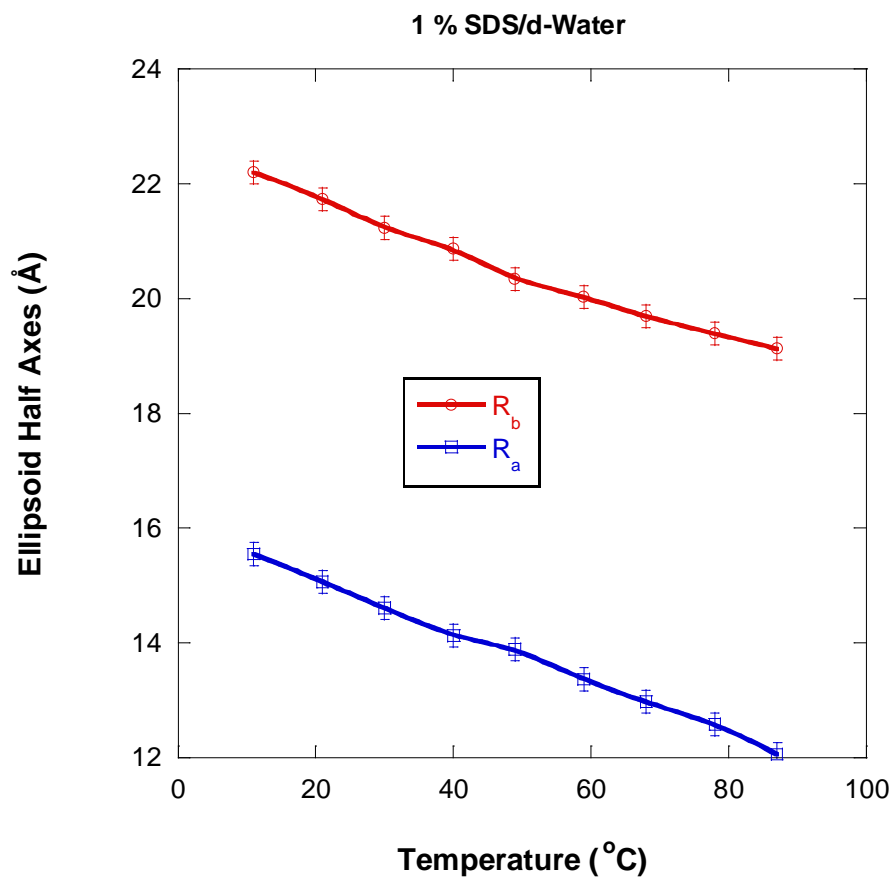
Figure 7: Variation of the ellipsoid micelles half axes with increasing temperature for the 1 % SDS sample. The lines going through the points are guides to the eye (smooth fitting).

The ellipsoidal micelle (oblate scattering particle) volume is estimated as $V_P = 4\pi R_a R_b^2 / 3$. This volume is seen (in Figure 8) to decrease consistently with increasing temperature and to increase with increasing SDS mass fraction. As temperature increases, the micelle volume decreases (so does the aggregation number) thereby yielding more (smaller) micelles. This is likely due to many factors that include softening of hydrogen-bonding of water molecules to the surfactant head groups and packing of the surfactant tails.
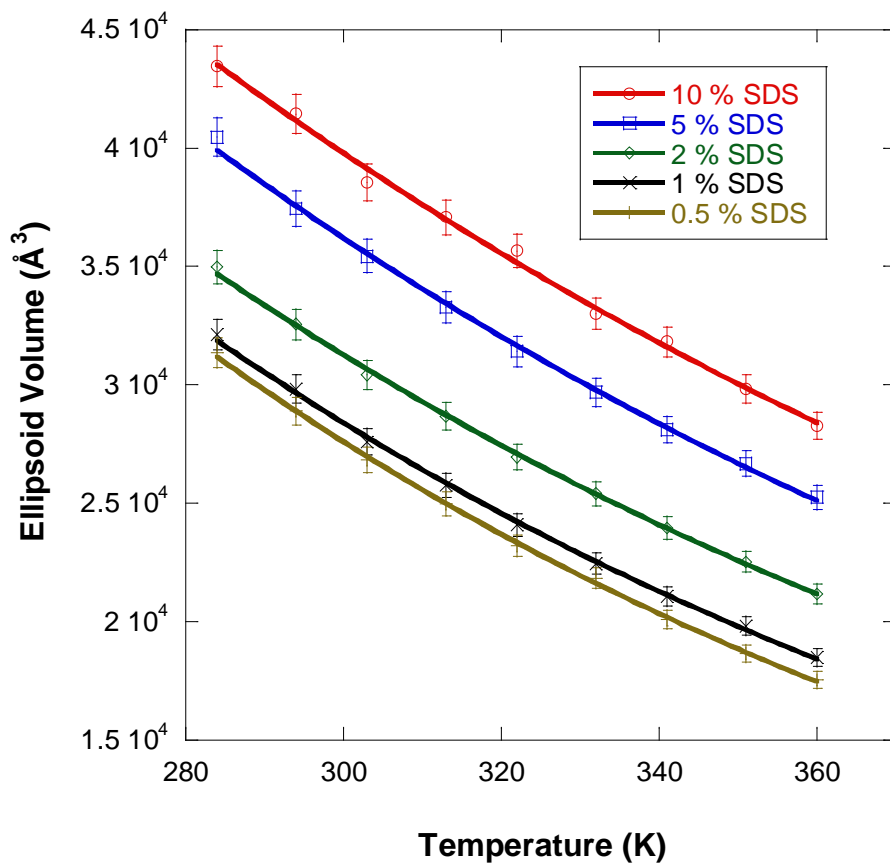
Figure 8: Variation of the ellipsoid micelle volume with increasing temperature for the various SDS mass fractions.

Fit results show that the charge on the micelles increases with SDS weight fraction (in Figure 9) as it should since the size of micelles increases with increasing SDS fraction. Micelle charges, however, decrease with increasing temperature since the micelle volume decreases with increasing temperature. This trend breaks down for the highest SDS mass fraction (20 %) sample. The same saturation trend at high SDS fraction was observed previously [Bezzobotnov et al, 1988]. Since the SDS molecule carries one electron charge on the ionized oxygen atom, the micelle charge scales with the micelle aggregation number.
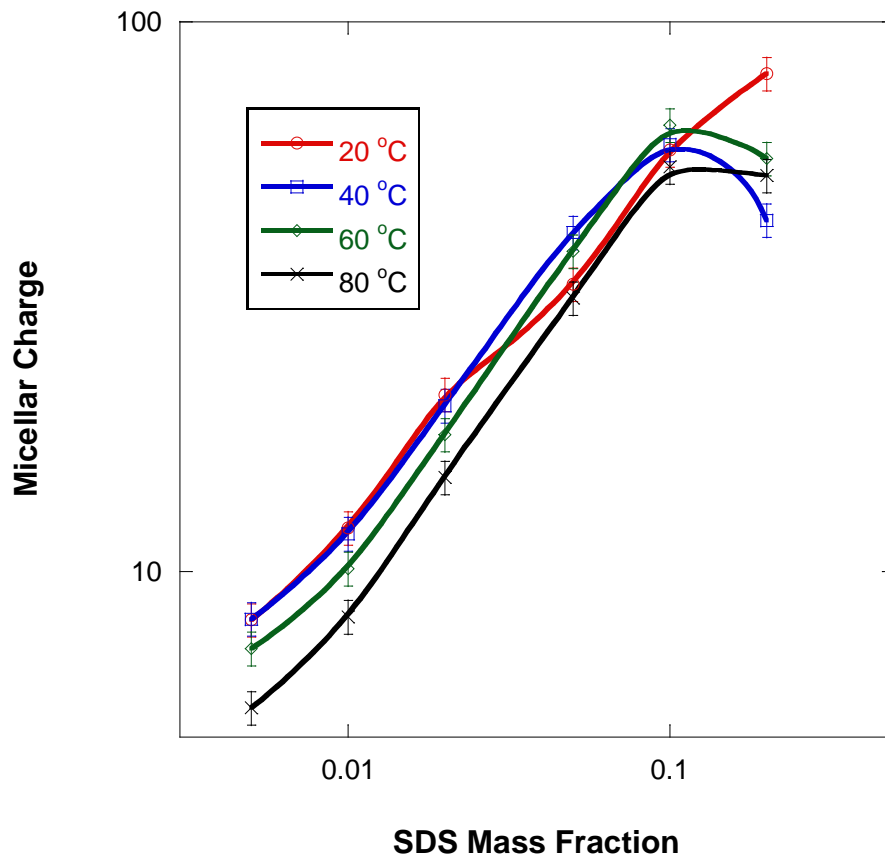
Figure 9 Variation of the micelle charge with increasing SDS mass fraction for various sample temperatures.

Sodium chloride (NaCl) salt was added to the 1 % SDS/d-water sample. Three salt fractions corresponding to 0.1 mol/L, 0.2 mol/L, and 0.5 mol/L were measured besides the no-salt (0 mol/L) sample. The minor half axis R_a is seen to increase, then flatten out (even slightly decrease) with increasing salt content while the major half axis R_b systematically increases (almost doubles from 0 mol/L to 0.5 mol/L salt content) as shown in Figure 10. Salt tends to screen charges on the micelle surface and to neutralize charges in the solvent. The observation that neutralized micelles are larger is not surprising since these are characterized by weaker Coulomb interactions that tend to repel SDS molecules from each other. Upon salt addition, the oblate micelles seem to grow laterally with not much increase in their thickness.
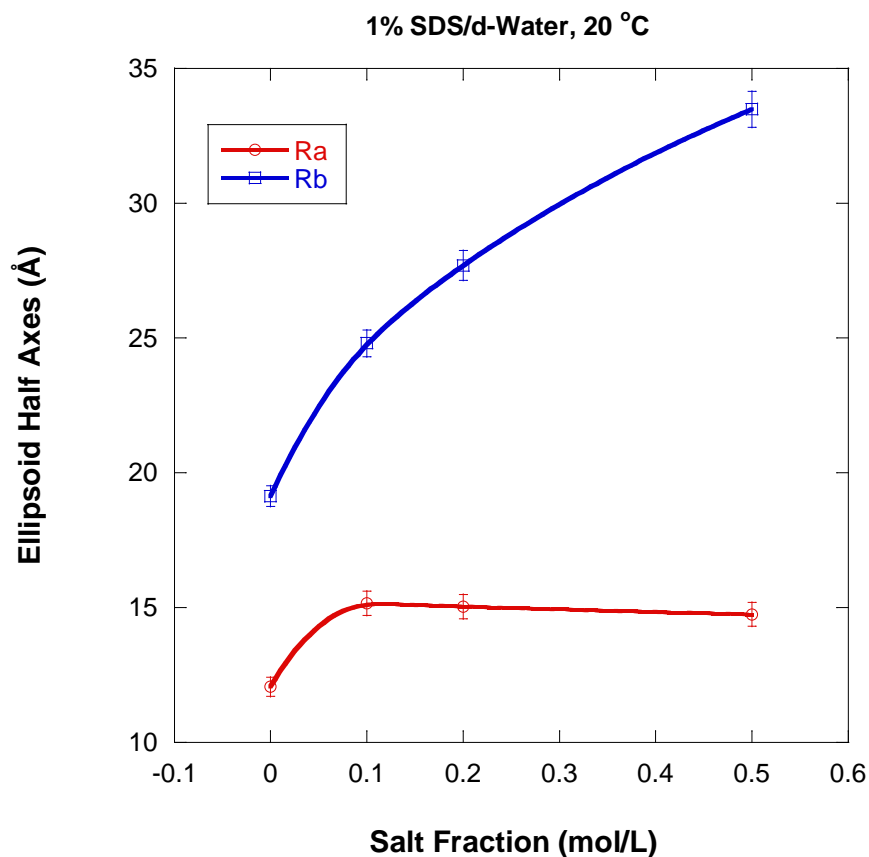
Figure 10 Variation of the ellipsoid micelles half axes with increase in NaCl salt content.

Fit results are reliable except for the 0.1 % SDS fraction sample. For all other samples, the ellipsoidal micelles volume fraction (from the fits) ϕ_{fit} is systematically lower than the SDS sample mixing volume fraction ϕ_{mix} (which is equal to the SDS mass fraction divided by its density which is around 1.01 g/cm^3). This means that not all SDS material takes part in micelle formation. Some of it remains homogeneously dissolved in the solvent. The temperature dependence is rather weak. Data for the lowest (0.1 %) and highest (20 %) SDS mass fraction samples break the trend. It should be mentioned that the measured contrast factor $\Delta\rho^2$ follows a similar trend.
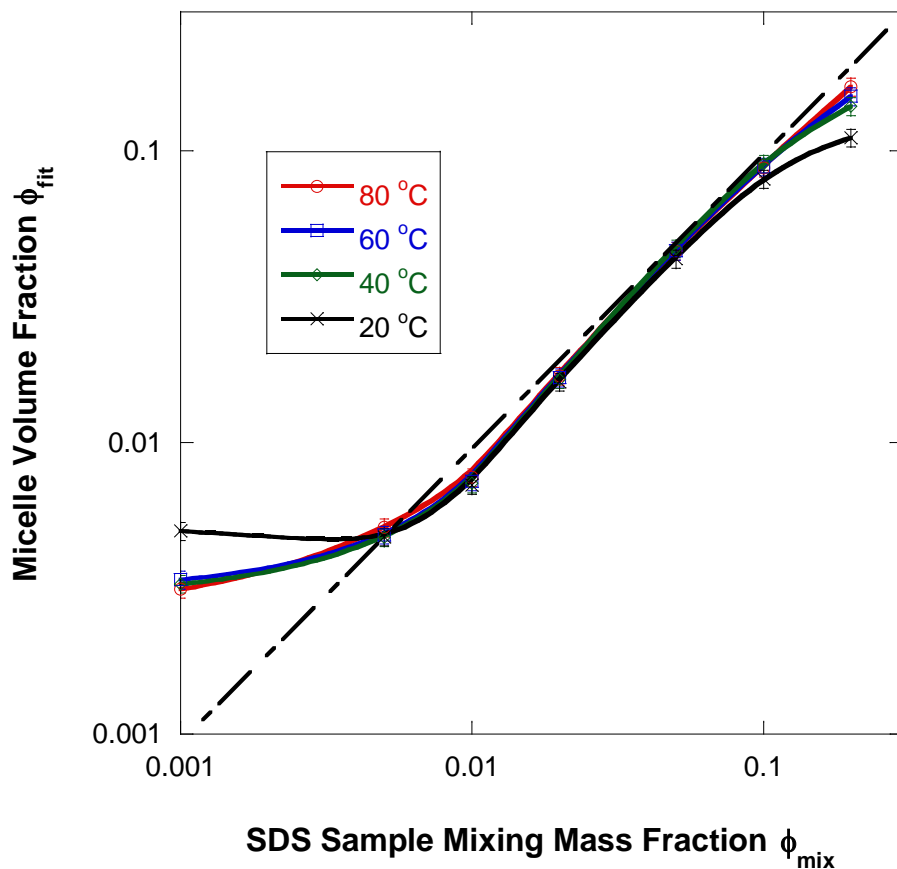
Figure 11: Variation of the fitted micelle volume fraction with the SDS sample mixing mass fraction at various temperatures. The dashed line represents a slope of one (equal fractions).

This last result suggests that some SDS molecules remain homogeneously dissolved in the solvent and do not participate in micelle formation (except for very low SDS fractions) as expected, since surfactants are soluble up to their critical micelle concentration (CMC) before micelles form in solution. A detailed material balance could be used to account for the relative SDS fraction that participates in micelle formation.

SUMMARY AND DISCUSSION

The SDS surfactant forms micelle structures in aqueous medium. Micelle particles were found to be mostly of an oblate ellipsoidal shape (compressed spheroid). Nonlinear least squares fits to an appropriate model corresponding to non-dilute mixtures of oblate spheroids yielded estimates for the minor and major micelle half axes. The 1 % SDS sample at 40 $^{\circ}$C, for example, is characterized by half axes of 14.1 $\pm$ 0.1 Å and 20.9 $\pm$ 0.1 Å respectively. At the highest SDS fraction of 20 % and lowest measured temperature of 10 $^{\circ}$C, another phase was observed. The two characteristic clues of a Bragg peak at high-

Q and a strong low-Q signal point to hydrated SDS crystals in agreement with the published phase diagram [Kekicheff et al, 1989]. .

The estimated micelle ellipsoid volume was found to decrease with increasing temperature and/or decreasing SDS fraction. Moreover, the micelle charge was also found to decrease with increasing temperature and/or decreasing SDS fraction as it should.

The oblate ellipsoid micelles half axes were found to increase with increasing NaCl salt addition. The minor half axis increases slightly then flattens out at 15 Å beyond 0.1 mol/L salt while the major half axis keeps on increasing up to 33 Å for 0.5 mol/L salt. The minor size is comparable to the SDS hydrocarbon tail size (fully extended size around 17 Å). Salt addition seems to screen charges on the micelles surface thereby allowing micelles to grow laterally while remaining of the thickness of one SDS close-to-stretched molecule.

The fitted micelle volume fraction ϕ_{fit} scales with the sample mixing SDS volume fraction ϕ_{mix} except at low (lower than 0.5 %) and high (higher than 10%) fractions. In the intermediate region around 1 % SDS fraction, it was concluded that not all SDS molecules participate in micelle formation; a small fraction remains homogeneously dissolved. For the 1 % SDS sample, at least 80 % of the SDS molecules are found to participate in micelle formation. The remaining 20 % are used to keep the dissolved SDS close to the CMC level.

THE SDS/D-WATER PHASE DIAGRAM

A phase diagram for the SDS/water system has been published [Kekicheff et al, 1989] based on calorimetric measurements. This phase diagram shows clearly the critical micelle formation line. Below it, hydrated SDS crystals form and above it, the various micelle phases are shown. These include spherical, cylindrical and lamellar micelles.
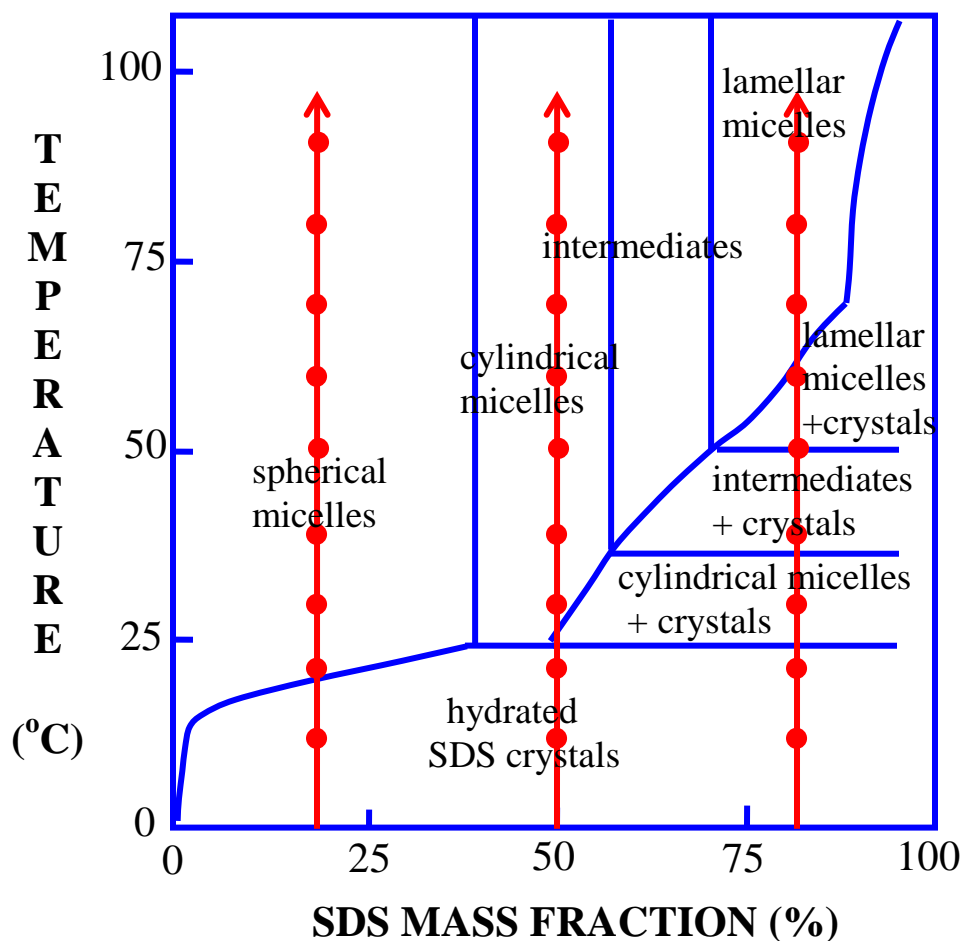
Figure 12: The SDS/water phase diagram. Red lines denote three recent series of measurements made on high fraction SDS samples.

REFERENCES

Bezzobotnov VY, Borbely S, Cser L, Farago B, Gladkih IA, Ostanevich YM, Vass S (1988) Temperature and Concentration Dependence of Properties of Sodium Dodecyl Sulfate Micelles Determined from Small-Angle Neutron Scattering Experiments, J. Chem. Phys. 92: 5738-5743

Kekicheff P, Grabielle-Madelmont C, Ollivon M (1989) Phase Diagram of SDS-Water System, Journal of Colloid and Interface Science, 131: 112-132

Borbely BS, Cser L, Vass S, Y.M. Ostanovich (1991) Small-Angle Neutron Scattering Study of Sodium Alkyl Sulfate Mixed Micelles, J. Appl. Cryst. 24: 747-752

Bergstrom M, Pedersen JS (1999) Structure of Pure SDS and DTAB Micelles in Brine Determined by Small-Angle Neutron Scattering, Phys. Chem., Chem. Phys. 1: 4437-4446

Prevost S, Gradizielski M (2009) SANS Investigation of the Microstructures in Cationic Mixtures of SDS/DTAC and the Effect of Various Added Salts, Journal Colloid and Interface Science, 337: 472-484

Yorelki K, Mitchell CA, Krishnamoorti R (2004) Small-Angle Neutron Scattering from Surfactant-Assisted Aqueous Dispersions of Carbon Nanotube", J. Amer. Chem. Soc., 126: 9902-9903

Nieh MP, Kumar SK, Fernando RH, Colby RH, Katsaras J (2004) Effect of the Hydrophilic Size on the Structural Phases of Aqueous Nonionic Gemini Surfactant Solutions, Langmuir, 20: 9061

Hammouda B (2010) Clustering in Polar Media, J. Chem. Phys. 133: 84901-1 to 5,

J.H. Hayter and J. Penfold (1981), "An Analytic Structure Factor for Macroion Solutions", Molecular Physics 42, 109-118

S. Kline (2006), "Reduction and Analysis of SANS and USANS Data using Igor Pro", J Appl. Cryst. 39, 895-900

R.C. Weast, Editor-in-Chief (1884), "CRC Handbook of Chemistry and Physics", 65th Edition, Page E57

RECENT SANS DATA FOR HIGHER SDS FRACTIONS

Our previous investigations mapped out SDS fractions up to 20 % in detail. Recent SANS data were taken from samples with higher SDS fractions (up to 80 %). Reduced data are shown. Detailed data analysis has not been performed yet.
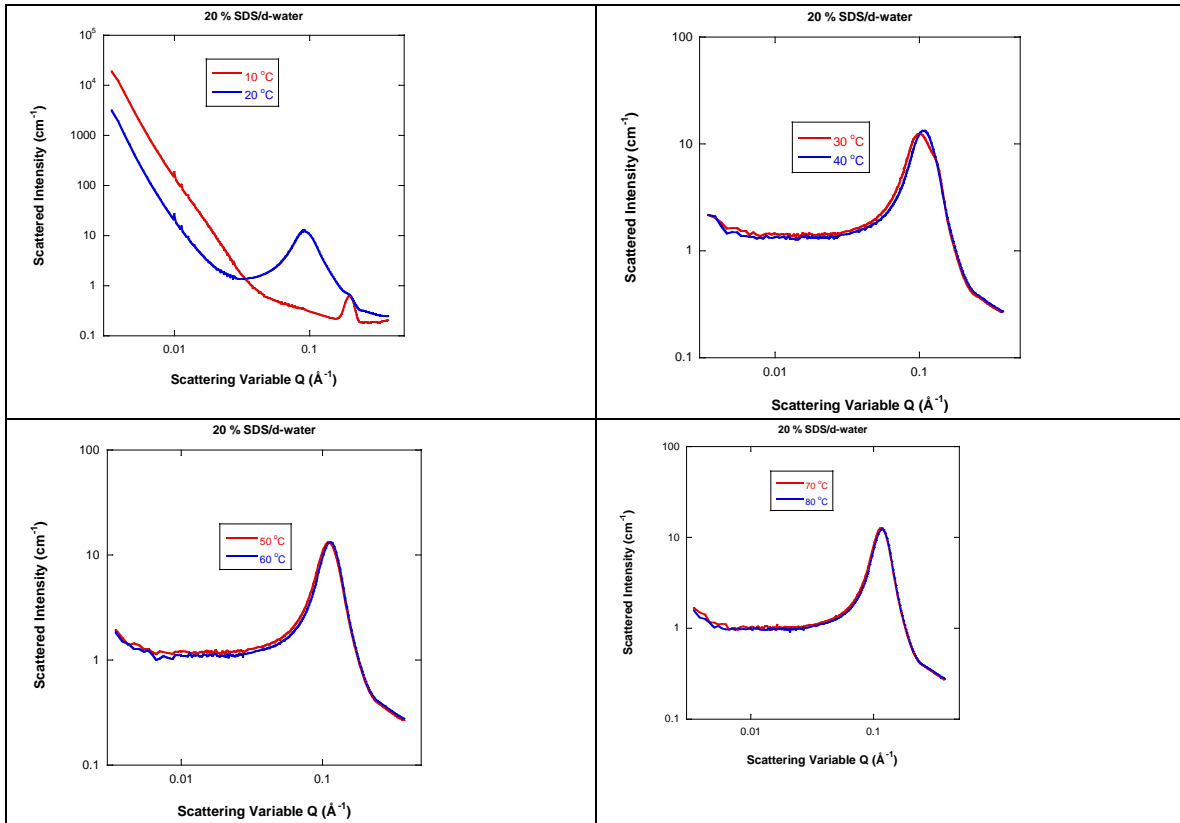

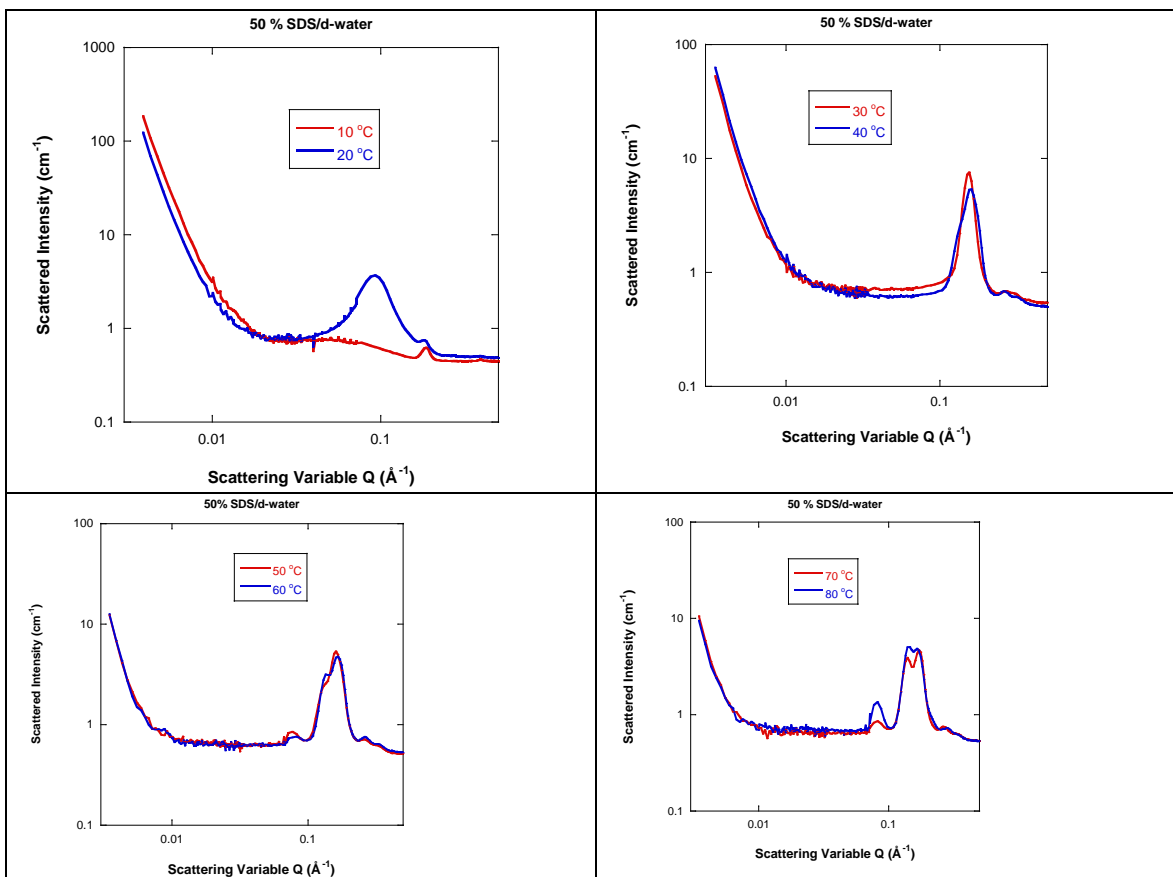Figure 13: SANS data from 20 % SDS/d-water at temperatures between 10 ^{o}C and 80 ^{o}C.

Figure 14: SANS data from 50 % SDS/d-water at temperatures between 10 $^{\circ}$C and 80 $^{\circ}$C.
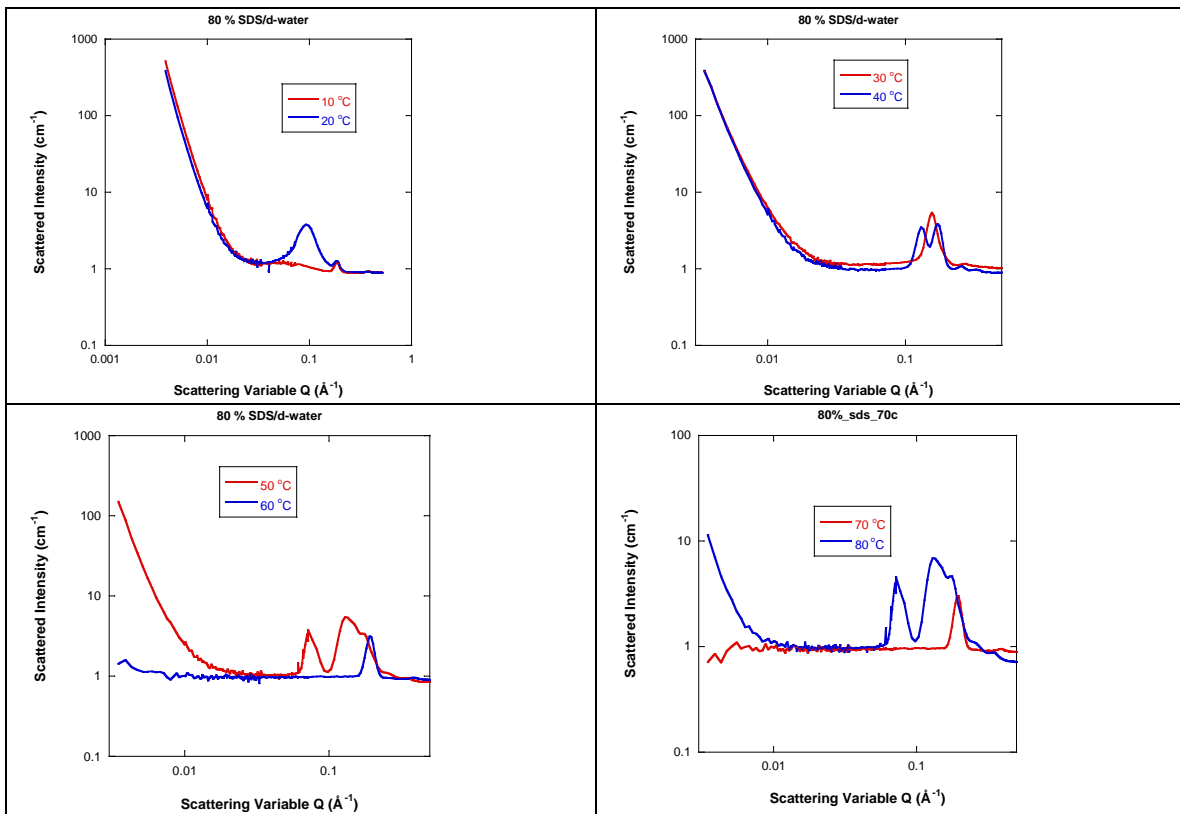
Figure 15: SANS data from 80 % SDS/d-water at temperatures between 10 ^{o}C and 80 ^{o}C.

POINTS TO THINK ABOUT

- Would a core-shell structural model yield more information than a uniform structure? What other structures are present?

- Check out the SDS phase diagram [Kekicheff et al, 1989] shown in Figure 12.

- Based on the recent SANS data (Figures 13-15), update the published phase diagram (Figure 12). Increasing figure magnification may be needed. As a hint, focus on clues from the data. Drastic changes in the trend points to a phase transition. Clearly how many phases can you identify? What are they?